ACS APPLIED MATERIALS & INTERFACES

Review

www.acsami.org

Recent Advances in Organic Transistor Printing Processes

Boseok Kang,[†] Wi Hyoung Lee,*[,‡] and Kilwon Cho*[,†]

[†]Department of Chemical Engineering, Pohang University of Science and Technology, Pohang 790-784, Korea

[‡]Department of Organic and Nano System Engineering, Konkuk University, Seoul 143-701, Korea

ABSTRACT: Recent progress in organic field-effect transistor (OFET) printing processes is reviewed, and a perspective on the future of the field is discussed. The principles underlying the OFET printing techniques are introduced according to two categories: direct write printing and transfer printing. A comprehensive overview of the use of printing techniques in OFET production processes is also provided. Considerations for improving OFET device performance using printing processes are explored. Prior to OFET commercialization, the OFET printing techniques must satisfy several requirements, as discussed here.

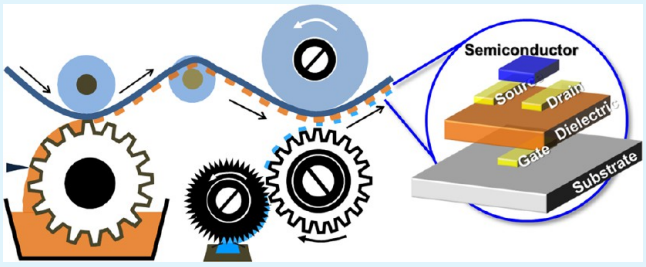

KEYWORDS: *organic field-effect transistors, printing, organic semiconductors, printed electronics, inkjet printing, transfer printing*

1. INTRODUCTION

Organic field-effect transistors (OFETs) have received considerable attention for their utility in the drivers of device display backplanes. OFETs have several advantages over their inorganic counterparts: OFETs are inexpensive and their components may be produced at high speeds. Printing processes that could enable the mass production of devices at relatively low costs are strongly desired in the industry.[1−3] Although conventional printing processes provide a good production platform, several technical barriers to the mass production of OFETs by printing processes remain.[4,5]

Figure 1 shows the layered structure of an OFET comprising a gate electrode, gate-dielectric, source/drain (S/D) electrodes, and semiconductor components. Depending on the sign of the gate bias, charge carriers can accumulate or be depleted at the semiconducting layer near the gate-dielectric. The accumulated charge carriers pass from the source to the drain electrode upon application of a potential difference across the electrodes. A goal in OFET processing is to construct each layer on a flexible substrate by consecutive printing processes. To achieve this goal, several requirements must be satisfied. First, the materials must be solution-processable in order for them to be applied to printing processes. Figure 2 shows the chemical structures of the printing materials discussed in this review. The semiconductor may be prepared from polymeric organic semiconductors, such as poly(3-hexylthiophene) (P3HT, Figure 2a) or small molecule organic semiconductors, such as triisopropylsilylethynyl pentacene (TIPS-pentacene, Figure 2b). An insulating polymer, such as poly(4-vinylphenol) (PVP) or poly(methyl methacrylate) (PMMA) is commonly used for the gate-dielectric. Low-voltage operation of an OFET requires the use of a high-k dielectric, such as an ionic liquid (1-ethyl3-methylimidazolium bis(trifluoromethylsulfonyl)imide, [EMIM][TFSI], Figure 2c).[6] The gate, source, and drain electrodes are commonly prepared from the water-soluble poly(3,4-ethylenedioxythiophene):poly(styrene sulfonate) (PEDOT:PSS) polymer because it is highly conductive and environmentally stable.[7]

Solvent orthogonality is important for the fabrication of multilayer films using printing processes. Because OFETs are layered structures, as shown in Figure 1, the solvent used during the top layer deposition should not damage the bottom layer. Thus, solvents must be carefully selected for the fabrication of each OFET layer in a printing process. Damage to the layers (i.e., swelling or dissolution of the bottom layer) may be avoided by using cross-linked polymers in the dielectric

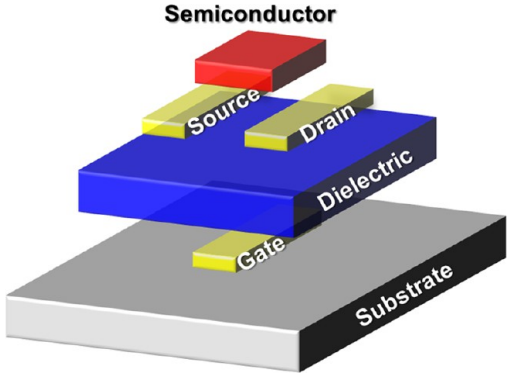

Figure 1. Schematic representation of the bottom-gate/bottom-contact OFET structure.

Special Issue: Forum on Advancing Technology with Organic and Polymer Transistors

Received: November 21, 2012
Accepted: February 11, 2013
Published: February 27, 2013

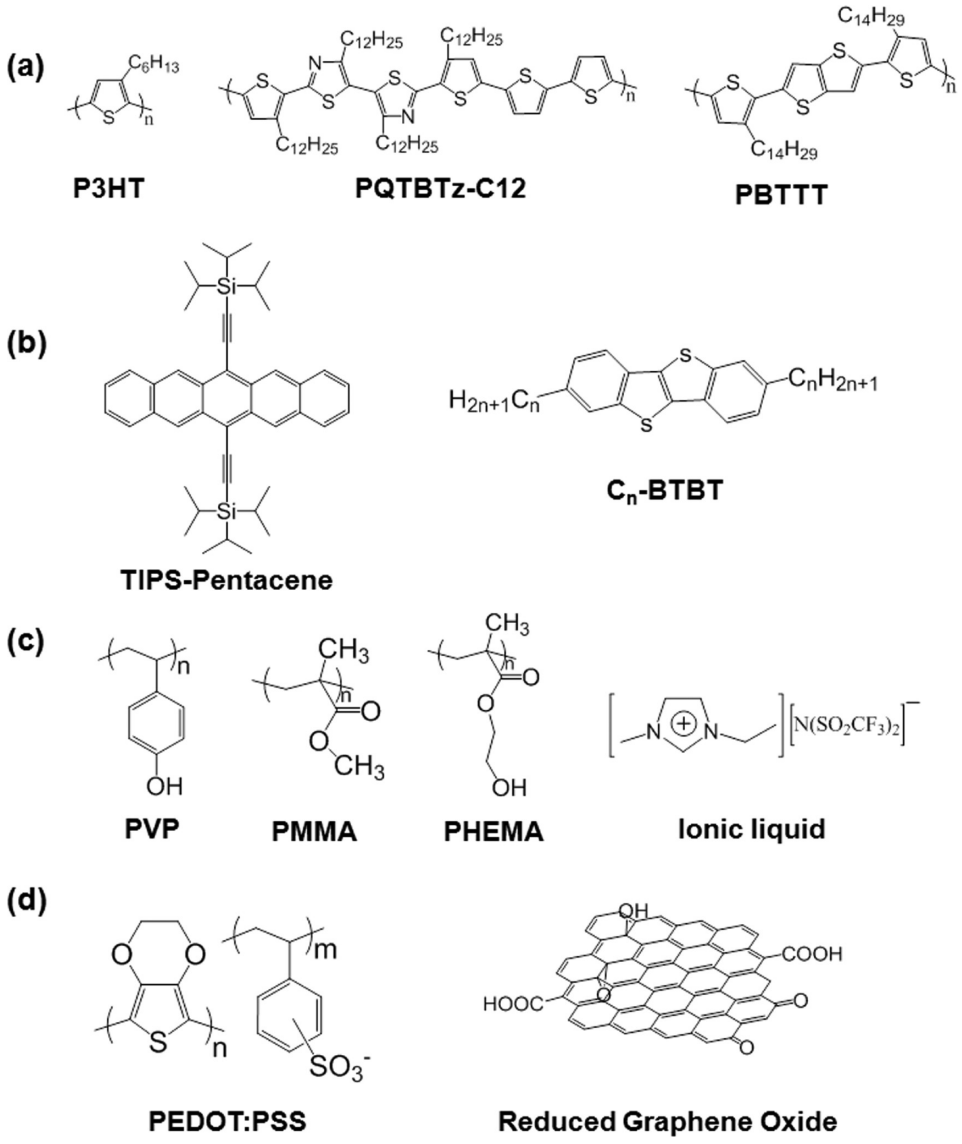

Figure 2. Chemical structures of the printing materials discussed in this review. (a) Polymeric organic semiconductors, (b) small molecule organic semiconductors, (c) insulator materials, (d) electrode materials.

layer.[8,9] Printing processes that do not damage the bottom layer must be developed. Precise layer patterning over a desired area is an important property of a printing process. Except for the dielectric layer, all layers must be patterned. Precision in the patterning of S/D electrodes is particularly essential because the OFET function is defined by the channel length and width. Because small channel length scales can increase the operating speed of a transistor, reducing the pattern size in printing processes is an important step toward enhancing the circuit speed.[10] Semiconducting layer may be isolated during precision patterning to reduce parasitic leakage current, thereby reducing the off-current in the device.[11] Similarly, the patterning of gate electrodes can reduce the gate leakage current. Layer alignment during patterning ensures proper device function. As shown in Figure 1, the deposition of S/D electrodes should be positioned in-line with the gate-electrode and semiconductor. Alignment is thus an important consideration in consecutive printing processes.

Although device materials and structures may be identical in design, device performances (including the field-effect mobility and on−off current ratio) can differ significantly according to the processing method. Because charge carriers pass through the semiconducting layer near the dielectric layer, the semiconductor−dielectric interface characteristics and the semiconductor crystallinity (or molecular ordering) must be optimized to achieve a high performance.[12−14] To this end, the morphological and structural characteristics of the organic semiconductors must be tuned during the printing process. Dielectrics must be uniformly deposited to reduce the gate leakage current. Source/drain electrodes should be sufficiently conductive and have an appropriate work function for the effective injection of charge carriers. Satisfaction of these requirements would yield functional transistors and facilitate the commercialization of OFETs manufactured by printing processes. The mere application of a printing method to OFET fabrication does not necessarily imply the successful preparation of properly functioning devices.

As OFET printing processes have become important in industry, they've become popular among researchers working on inorganic and organic electronic devices. Several well-written review articles covering printing methodologies are available.[2,4,6,11,15] Despite the widespread use of printing

methods in the research-scale production of OFETs, the processes themselves are not well understood. Certain technical issues have been neglected in previous reports, and discussions have mainly focused on the methods used in the fabrication processes. Significant variations in performance are observed among devices prepared from the same materials using the same printing method. A critical review of OFET printing processes is, therefore, required. The commercialization of OFETs depends largely on the development of appropriate printing processes.

This review discusses recent advances in OFET printing processes in an effort to understand the current status and future perspectives on the field. Printing processes may be categorized according to the characteristic procedures of the printing process. Patterning via ink ejection in a noncontact manner is categorized as "direct write printing". Inkjet printing, aerosol-jet printing, spraying, and vapor-jet printing are included in this category, and these methods will be introduced in section 2. "Transfer printing", on the other hand, refers to the patterning of materials on a target substrate using a transfer medium (i.e., a mold, stamp, or roll). In transfer printing, the contact between the transfer medium and the target substrate determines the success of pattern formation. Microcontact and -transfer printing, laser-induced forward printing, gravure printing, flexography printing, and offset printing are included in this category and will be reviewed in section 3. Although some printing processes straddle the two categories, this classification system is useful for explaining the fundamental principles underlying OFET printing processes and fabrication procedures.

2. DIRECT WRITE PRINTING

Direct write printing utilizes specialized equipment that efficiently ejects the printed materials. For example, inkjet printing uses an inkjet nozzle to dispense materials,[15] whereas aerosol-jet or spray-printing techniques use a valve and pipe to paint materials from a pressurized container.[6] Direct write printing methods are very efficient for use in consecutive printing processes because direct patterning may be achieved in a noncontact manner, reducing the risks associated with contaminating the dispensing nozzle. The pattern accuracy, on the other hand, may be hampered by unwanted spreading and drying of the printed ink.[1] The precise deposition of materials over a desired area is, therefore, time-consuming. Several methods have been developed to alleviate these problems, and these will be introduced in the following section.

2.1. Inkjet Printing. Inkjet printing is a well-known digital printing process used in the fabrication of small patterns. This noncontact, additive, direct-write patterning process uses nozzle and piezoelectric control systems to eject small volumes of ink. Figure 3a shows a schematic diagram of the inkjet printing process, consisting of ink ejection, flight, impact, spreading, and drying. The ink properties (i.e., the solvent, ink concentration) and the substrate surface properties must be optimized to achieve well-defined patterns. The solvent and ink concentration, in particular, must be carefully selected when used in consecutive ejection printing processes in order to avoid nozzle clogging, which can interrupt a continuous inkjet printing process. The substrate surface properties and the ink properties can critically affect the drying behavior of a droplet, which determines the final morphology and structure of the deposited ink spot. The right inset of Figure 3a shows an image of a typical coffee stain pattern formed in an inkjet-printed polymer

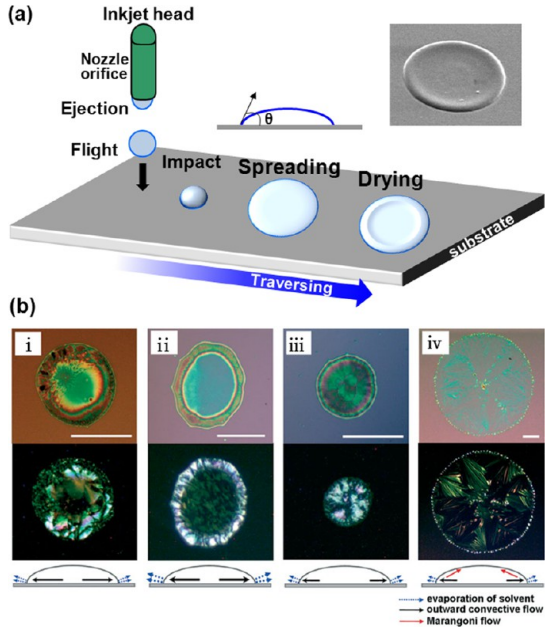

Figure 3. (a) Schematic diagram showing the inkjet printing process. The right/top image shows an SEM image of an inkjet-printed PEDOT:PSS electrode. (b) OM (top) and polarized OM (middle) images of inkjet-printed TIPS-pentacene droplets prepared using a variety of solvent compositions: (i) chlorobenzene, and several mixed-solvents containing chlorobenzene and 25 vol% (ii) hexane, (iii) *o*-dichlorobenzene, and (iv) dodecane. The bottom columns show a schematic diagram of the evaporation-induced flow in a droplet. The scale bar indicates 50 μm. Reproduced with permission from ref 19. Copyright 2008 Wiley.

film. This coffee stain effect arises from the outward convective flow within a droplet and prevents the materials from depositing uniformly.[16] The overall process must be optimized to obtain a desired pattern via inkjet printing.

2.1.1. Semiconductor. Inkjet printing is widely used for fabricating source/drain electrodes and semiconducting layers in OFETs. The functional differences between semiconductors and source/drain electrodes impose different requirements on the inkjet printing parameters of the materials. For inkjet-printed organic semiconductors, it is important to control the morphological/structural characteristics during the drying process because these characteristics critically affect the electrical properties of an OFET.[17,18] Figure 3b shows OM and polarized OM images of TIPS-pentacene droplets, revealing the morphological and structural development over time after the inkjet printing process.[19] The flow in the droplets differed significantly, depending on the solvent. As a single solvent, chlorobenzene produced typical coffee stain images with less ordered TIPS-pentacene crystals (i). The addition of a cosolvent intensified (ii) or reduced (iii) the coffee stain effects. Interestingly, the use of dodecane, with a high boiling point and a low surface tension, as a cosolvent yielded highly crystalline TIPS-pentacene crystals as a result of surface-tension-driven Marangoni flow (iv). The field-effect mobility of the TIPS-pentacene FETs increased by 2 orders of magnitude, yielding a mobility of 0.12 $cm^2\ V^{-1}\ s^{-1}$ for the chlorobenzene/dodecane cosolvent system. A mixed solvent approach is also desirable for increasing the crystallinity of other organic semiconductors, 2,7-dioctyl benzothieno benzothiophene (C_8–BTBT).[20] Figure 4a illustrates the "double shot" inkjet printing process, involving the inkjet printing of an antisolvent (or nonsolvent), followed

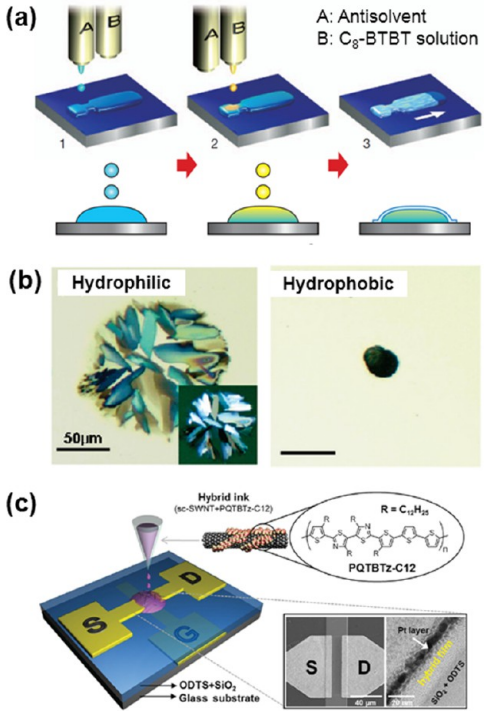

Figure 4. (a) Schematic diagram showing the fabrication of C_8–BTBT single crystals. Antisolvent A was inkjet-printed (Step 1), and then solution B was overprinted to form intermixed droplets confined to a defined area (Step 2). Single crystals nucleated and grew at the liquid–air interfaces (Step 3). Reproduced with permission from ref 20. Copyright 2011 Nature Publishing Group. (b) OM images of the inkjet-printed TIPS-pentacene droplets on a UV-ozone-treated SiO_2 substrate (left) and an OTS SAM-modified SiO_2 substrate (right). Reproduced with permission from ref 21. Copyright 2009 American Chemical Society. (c) Printed hybrid ink composed of SWNTs and PQTBTz-C12. The right inset shows SEM and cross-sectional TEM images of the active layer. Reproduced with permission from ref 26. Copyright 2012 American Chemical Society.

by printing of the C_8–BTBT solution. The spatial confinement of C_8–BTBT induced crystal nucleation and growth at the liquid–air interface, leading to the formation of single crystals after solvent evaporation. FETs prepared from these single crystals displayed field-effect mobilities as high as 16.4 $cm^2\ V^{-1}\ s^{-1}$.

In addition to controlling the solvent, the self-organization of organic semiconductor materials during drying can be modulated by the substrate surface properties. Cho and co-workers examined the morphological and structural characteristics of inkjet-printed TIPS-pentacene as a function of the substrate wettability.[21] On a hydrophilic UV–ozone-treated SiO_2 substrate, the hydrodynamic flow toward the pinned contact line induced self-assembly of the TIPS-pentacene molecules, resulting in highly crystalline TIPS-pentacene crystals (Figure 4b, left). On the other hand, small low-crystallinity TIPS-pentacene agglomerates formed on a hydrophobic SiO_2 substrate modified with an octadecyltrichlorosilane (OTS) self-assembled monolayer (SAM, Figure 4b, right). This behavior was attributed to the formation of aggregates via depinning of the contact line. The substrate wettability can be controlled to achieve the selective patterning of organic semiconductors. Kim et al. fabricated TIPS-pentacene single crystals over a defined area by inkjet printing the solution onto a substrate with a controlled and patterned wettability.[22] The hydrophilic region was patterned using UV–ozone treatment of an OTS-modified SiO_2 substrate. Subsequent inkjet printing of a TIPS-pentacene solution selectively formed single crystals over the hydrophilic region. A fabricating bank designed for the selective deposition of materials provides another novel method for increasing the patterning accuracy. Such a bank is normally fabricated using a photoresist following photolithographic processes. Kjellander et al. prepared a self-aligned bank directly by inkjet printing TIPS-pentacene ink onto a thin insulating polymer-coated substrate.[23] Here, the solvent used to prepare the TIPS-pentacene solution dissolved the insulating polymer, leading to the formation of TIPS-pentacene crystals within the insulating polymer bank. Remarkably, this process increased the accuracy of the TIPS-pentacene patterning process. The field-effect mobility of an FET depends on the thickness and molecular weight of the insulating polymer. A mobility of 0.8 $cm^2\ V^{-1}\ s^{-1}$ may be obtained under optimized conditions.

Polymeric semiconductors have been widely used in the preparation of inkjet-printed organic semiconductors. In most cases, the performances of FET devices prepared with inkjet-printed organic semiconductors are inferior to those of FETs prepared with spin-cast organic semiconductors.[24,25] The performance differences mainly arise from the low crystallinity of inkjet-printed organic semiconductor films. This problem was addressed by Kim et al. by blending single-walled carbon nanotubes (SWNTs) in a poly(didodecylquaterthiophene-altdidodecylbithiazole (PQTBTz-C12) solution (Figure 4c).[26] By separating the semiconducting SWNTs from the metallic SWNTs and adding semiconducting SWNTs to the PQTBTz-C12 solution, the field-effect mobility of the inkjet-printed OFETs increased greatly without shifting the threshold voltage. Cho and co-workers used a P3HT/polystyrene (PS) blended ink to fabricate high-performance inkjet-printed OFETs.[27] By manipulating the solvent properties, P3HT nanowires embedded in a PS matrix could be successfully fabricated using an inkjet printing process. This structure very efficiently increased the environmental stability while maintaining a high field-effect mobility and an on/off current ratio.[27,28] Compared to FETs prepared with inkjet-printed polymeric semiconductors, FETs prepared with inkjet-printed small molecule semiconductors typically exhibit significant device-to-device performance variations.[17] New approaches to reducing device-to-device variation in small molecule semiconductor FETs are required. Madec et al. increased reproducibility of inkjet-printed TIPS-pentacene FET devices using a blend ink composed of TIPS-pentacene and an insulating polymer.[29] They observed that the stable ejection of the blend ink decreased the device-to-device variations. Similarly, James et al. fabricated highly anisotropic TIPS-pentacene crystals using a TIPS-pentacene/PS blend ink.[18] They found that PS did not disrupt the π–π stacking among TIPS-pentacene molecules, and it contributed to the formation of a uniform morphology and high active layer coverage.

2.1.2. Source/Drain Electrodes. Inkjet printing is a very efficient method for fabricating S/D electrodes. A standard picoliter inkjet printer produces a minimum pattern size of around 20 μm. The feature size in electrode lines may be reduced using several methods. Figure 5a illustrates a method for increasing the deposition accuracy using a polymer bank.[7] Because polyimide polymers are hydrophobic, the bank prevents the PEDOT:PSS ink for spreading and blending, thereby enabling the fabrication of 5 μm channels. Another method for fabricating fine patterns involves the dewetting of a

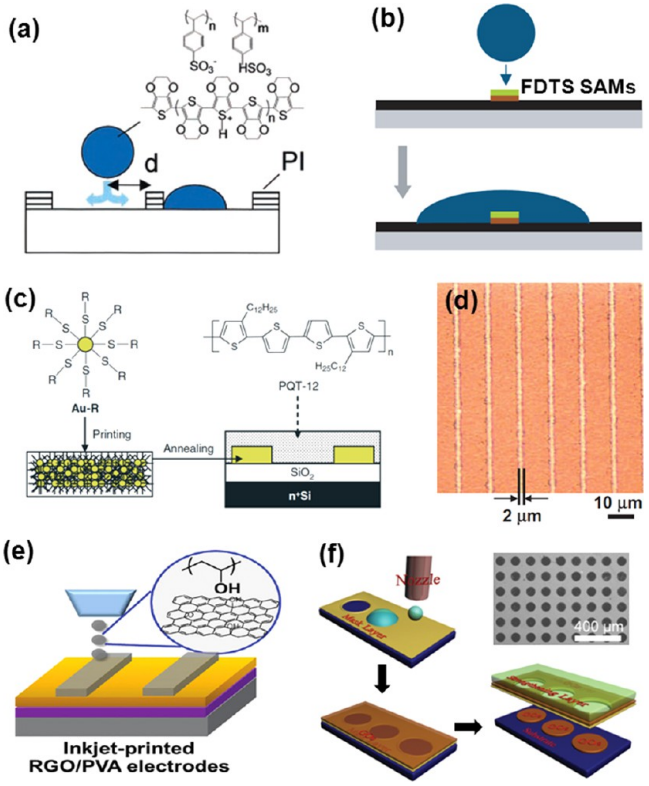

Figure 5. (a) Schematic diagram of the inkjet printing process on a patterned substrate. Reproduced with permission from ref 7. Copyright 2000 AAAS. (b) An inkjet patterning process involving the use of dewetting on a FDTS SAM-treated substrate. Reproduced with permission from ref 30. Copyright 2004 Nature Publishing Group. (c) PQT-12 transistors prepared with Au nanoparticle source/drain electrodes. Reproduced with permission from ref 33. Copyright 2005 Wiley. (d) Ag electrode pattern fabricated using a sub-femtoliter inkjet printing system. Reproduced with permission from ref 38. Copyright 2008 National Academy of Sciences U.S.A. (e) Reproduced with permission from ref 41. Copyright 2012 American Chemical Society. (f) Reproduced with permission from ref 42. Copyright 2012 Wiley.

polymer solution. Sirringhaus and co-workers used 1H, 1H, 2H, 2H-perfluorodecyltrichlorosilane (FDTS) SAMs to fabricate S/D electrodes (Figure 5b).[30] The surface energy barrier was used to induce dewetting of a PEDOT:PSS layer, and a 500 nm pattern size was achieved using this process. Similarly, CF_4 plasma treatment of PEDOT:PSS induced dewetting of subsequently deposited PEDOT:PSS droplets.[31] S/D electrode pattern size reduction was used to fabricate high-speed circuits that operated at high frequencies. In addition to decreasing the electrode line feature size, OFET performance may be enhanced by tuning the conductivity of the PEDOT:PSS electrodes. Cho and co-workers added dimethyl sulfoxide (DMSO) to a PEDOT:PSS solution to increase the conductivity of an inkjet-printed PEDOT:PSS electrode.[32] The electrical properties of the P3HT FETs were enhanced because of an increase in the S/D electrode conductivity.

Inkjet printing of metal nanoparticles can provide robust, highly conductive patterned S/D electrodes. Wu et al. used n-butanethiol-functionalized Au nanoparticles as S/D electrodes (Figure 5c).[33] After inkjet printing, thermal treatment at 200 °C converted the Au particles to a uniform Au film. Poly(didodecylquaterthiophene) (PQT-12) FETs with inkjet-printed Au contacts exhibited high field effect mobilities of 0.15 $cm^2\ V^{-1}\ s^{-1}$. Several groups have tried to reduce the sintering temperature of inkjet-printed metal nanoparticles by using different precursors.[34−37] These efforts are particularly important in the fabrication of S/D electrodes prepared from metal nanoparticles on flexible plastic substrates. The feature size of an inkjet-printed metal nanoparticle electrode was reduced using a femtoliter inkjet printer. Sekitani et al. succeeded in fabricating 2 μm Ag lines by inkjet printing Ag nanoparticles and sintering at 130 °C (Figure 5d).[38]

Carbon materials can be used to prepare S/D electrodes in OFETs.[39] Although carbon nanotubes (CNTs) may be used in principle, nozzle clogging poses a significant barrier to the use of CNTs in inkjet-printable electrodes. Solution-processable graphene (or chemically derived graphene) can be used to prepare inkjet-printed S/D electrodes. Because exfoliated graphene oxide is highly insulating, a reduction process is needed to recover the conductivity of graphene, and reduced graphene oxide (RGO) is generally used to prepare inkjet-printed graphene electrodes.[40] The printing reproducibility, patternability, and conductivity of RGO must be optimized for the preparation of inkjet-printed S/D electrodes. Reproducibility depends on the properties of an RGO dispersion. Cho and co-workers added polyvinyl alcohol (PVA) to an RGO solution to enhance the RGO dispersibility (Figure 5e).[41] A high dispersibility leads to stable RGO ejection properties, thereby increasing the reproducibility of an inkjet printing process. Liu and co-workers used coffee-ring lithography to resolve the patternability issues.[42] Inkjet-etched micro wells were used to pattern RGO (Figure 5f). The patterned RGO S/D electrodes were then used to fabricate high-performance OFETs. The conductivity depends strongly on the graphite oxidation and exfoliation processes and/or the method used to reduce graphene oxide. The reader is referred to other review articles that discuss the production of RGO in greater detail.[43−45]

2.2. Aerosol-Jet and Spray Printing. Aerosol-jet printing is a commercialized digital printing method used to deposit a variety of materials. "Aerosol" means a suspension of solid or liquid particles in a gas. This intermediate material state is usually prepared using an ultrasonic aerosol generator. Figure 6a shows a schematic diagram of the aerosol-jet printing process. Aerosolized particles from a pressurized container are ejected toward a target substrate through the pipe used to transport the aerosol. This method can be applied toward the production of the semiconductor, insulator, and electrode OFET components. Cho et al. fabricated all-printed FETs on a plastic substrate using aerosol-jet printing (Figure 6b).[6] They used Au nanoparticles, P3HT, ionic liquids ([EMIM][TFSI]) and PEDOT:PSS as S/D electrodes, semiconductors, dielectrics, and gate-electrodes, respectively. Importantly, these components were all successfully fabricated via aerosol-jet printing, and the low-voltage FETs fabricated according to this process displayed high performances.

Spray printing is an extremely low cost technique for depositing a variety of materials. Commercially available airbrush kits may be used for such a setup. The operating principle underlying spray printing is very similar to that underlying aerosol-jet printing. Spray printing, in combination with a shadow mask, can be used to fabricate S/D electrodes. Cho and co-workers fabricated spray-patterned PEDOT:PSS S/D electrodes (Figure 6c).[46] They observed that the substrate temperature was critical for preparing fine electrode patterns. The patterned S/D electrodes were used to fabricate high-

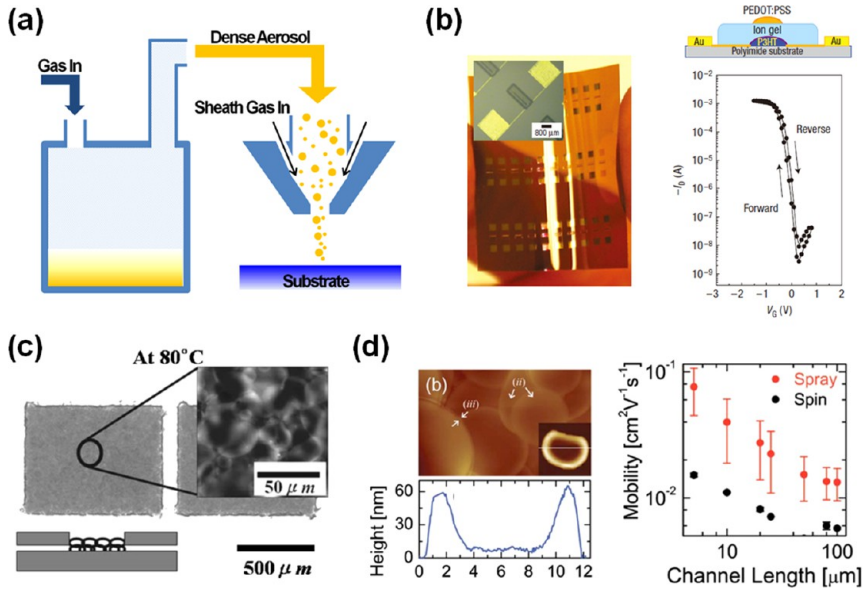

Figure 6. (a) Schematic drawing showing the aerosol printing process. (b) OM image (left), device structure (right/top), and the electrical properties (right/bottom) of an aerosol-printed transistor array prepared on a plastic substrate. Reproduced with permission from ref 6. Copyright 2008 Nature Publishing Group. (c) PEDOT:PSS S/D electrodes fabricated by spray printing. Reproduced with permission from ref 46. Copyright 2008 American Institute of Physics. (d) AFM image and height profile of a P3HT film fabricated by spray printing (left). Comparison of the field-effect mobilities in P3HT transistors prepared via two different P3HT deposition processes (right). Reproduced with permission from ref 47. Copyright 2010 American Institute of Physics.

performance OFETs. Spray printing can also be used to deposit organic semiconductors. Chan et al. used spray-coated P3HT as the active layer in an OFET (Figure 6d).[47] Although spray-coated P3HT films are very rough, FETs prepared with such films exhibited higher field-effect mobilities than FETs prepared with spin-coated films. The molecular orientations of the P3HT (i.e., the transport-relevant π-conjugated backbone plane) in spray-coated films were similar to the molecular orientations in spin-coated films.

2.3. Organic Vapor-Jet Printing (OVJP). Organic vapor-jet printing (OVJP), similar to organic molecular beam deposition (OMBD), is a vapor version of inkjet printing. In the OVJP process, a hot inert carrier gas (e.g., helium or nitrogen) is seeded with organic vapor and then expanded through a microscopic nozzle to form a highly collimated gas jet (Figure 7a).[48] The jet impinges on a cold substrate and the light carrier gas molecules quickly disperse while the organic molecules condense on the surface. The OVJP is free from the solvent orthogonality problem because it does not use organic solvent. The pattern resolution may be controlled directly by the nozzle size, nozzle−substrate gap, and the pressure and type of carrier gas. The mechanism by which polycrystalline pentacene films form during OVJP is schematically illustrated in Figure 7b. Islands nucleate and grow via the addition of vapor molecules that arrive at the substrate.[49] The mutual shadowing of islands during growth produces a tilted grain. Pentacene transistors printed by OVJP exhibited field-effect mobilities of 0.25 $cm^2\ V^{-1}\ s^{-1}$ and on−off current ratios of 7×10^5. Yun et al. added a digital mode to the OVJP setup by applying a continuous flow of vapor during nozzle movement.[50] The performances of OFETs fabricated using the digital-mode OVJP (D-OVJP) method were comparable to those of OFETs prepared by conventional OVJP methods (Figure 7c). The high spatial resolution of the OVJP method was demonstrated by reproducing the famous painting "Girl with a pearl earring" by means of pixel-to-pixel deposition, controlled by D-OVJP (Figure 7d).

Molecular jet (MoJet) printing, a digital printing approach similar in nature to the D-OVJP method, was investigated by Chen et al.[51] To achieve flux-on-demand analogous to the concept of drop-on-demand in inkjet printing, the authors fabricated a print head using a microelectro-mechanical system (MEMS). This print head, along with a moving stage, were used to deposit the vapor flux in a desired position. The MoJet technique was used to fabricate pentacene FETs with device performances comparable to those of FETs fabricated by conventional methods.

2.4. Screen-Printing. Screen-printing, a technique intermediate between direct write printing and transfer printing, is a common conventional printing method. In this technique, ink is pressed with a squeegee onto a woven mesh (screen) onto which is fixed an ink-blocking stencil, as shown in Figure 8a. The ink is then printed onto a substrate through the open areas of the mesh. The simplicity of the process enables printing of a wide variety of inks onto any type of substrate. An example of screen-printing is shown in Figure 8b, which displays the printing of poly(2-methoxy-5-(2′-ethylhexyloxy)-1,4-phenylenevinylene) (MEH-PPV) onto an indium tin oxide (ITO)-coated glass substrates.[52] In the early stages of OFET research, Garnier et al. described the preparation of all-polymer FETs in which electrodes were deposited by screen-printing.[53] Bao and co-workers demonstrated the preparation of organic transistors in which all essential components were screen-printed directly onto a plastic substrate.[54] Rogers et al. described screen-printed OFETs in combination with micromolded carbon paint for the preparation of S/D electrodes.[55] More recently, OFETs with a channel length of 30 μm were fabricated by Lim et al. (Figure 8c).[56] Screen-printed metal electrodes were prepared from a solution containing Ag nanoparticles mixed with carbon black to achieve a high conductivity and work function. The authors reported a field-effect mobility of up to 7×10^{-2} $cm^2\ V^{-1}\ s^{-1}$

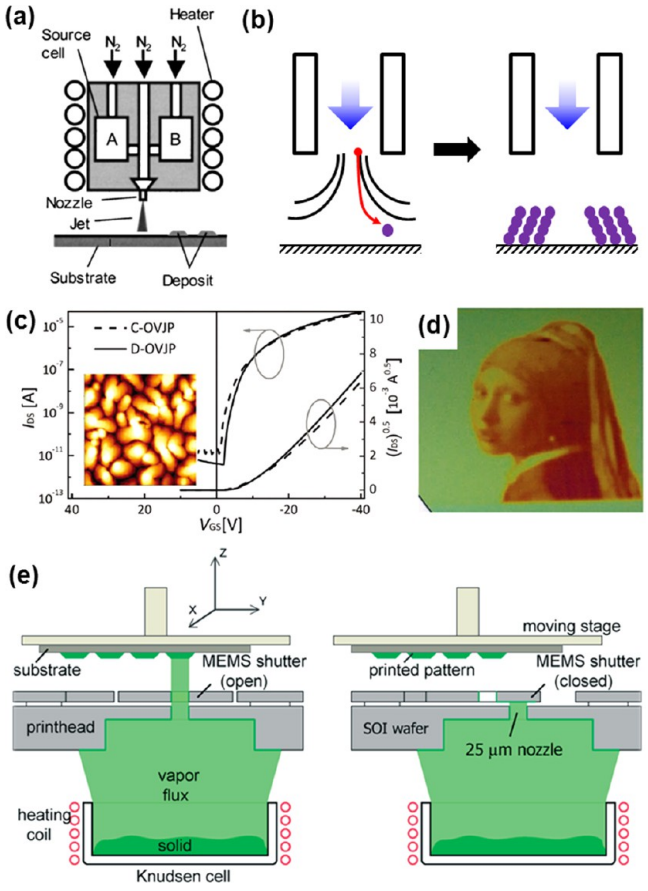

Figure 7. (a) Schematic diagram showing the setup used in organic vapor-jet printing (OVJP) equipment. Reproduced with permission from ref 48. Copyright 2004 Wiley. (b) Flow and movement of the target materials in a chamber. (c) Electrical properties of pentacene transistors fabricated by OVJP. C-OVJP, conventional mode; D-OVJP, digital mode. Reproduced with permission from ref 50. Copyright 2012 Wiley. (d) Images drawn using an OVJP-deposited pentacene film. Reproduced with permission from ref 50. Copyright 2012 Wiley. (e) Schematic drawing showing the molecular jet printing equipment. When the MEMS shutter is open, the vapor flux can pass through the nozzle, reach the substrate, and form a deposited pattern on the substrate. When the shutter is closed, the vapor flux is blocked. Reproduced with permission from ref 51. Copyright 2007 Wiley.

using pentacene as the semiconducting layer. A low-cost patterning method compatible with vacuum deposition methods was investigated by Someya and co-workers.[57] They used a screen-printed epoxy shadow mask to precisely control the device dimensions (Figure 8d). After vacuum evaporation of a pentacene layer, a masking resist patterned by screen-printing was peeled off from the base film without inducing mechanical damage to the lower structures. The resultant device displayed a field-effect mobility of 0.4 $cm^2 V^{-1} s^{-1}$ and an on−off current of 1×10^5, indicating that the solution-based patterning of a shadow mask did not increase the leakage current through the underlying polymer insulator.

3. TRANSFER PRINTING

Transfer printing provides an alternative approach to the production of organic transistors. This printing method uses a transfer medium in which materials are transferred via direct contact between the material and the target substrate. This high-throughput, low-cost, and simple printing process is quite

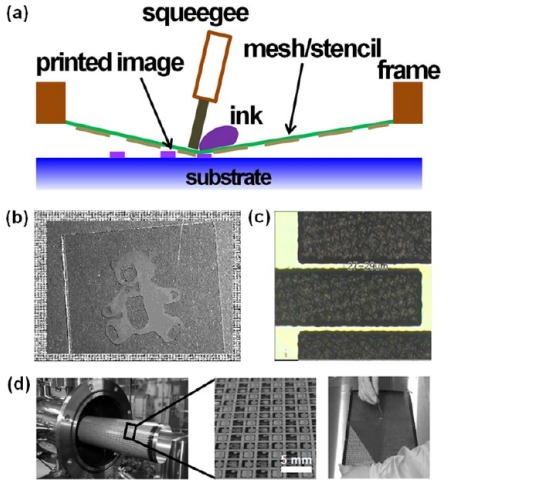

Figure 8. (a) Schematic drawing of the screen-printing process. (b) Photograph of a photoluminescent image of a screen-printed MEH-PPV polymer logo. Reproduced with permission from ref 52. Copyright 2000 Wiley. (c) Ag nanoparticle/carbon black electrodes fabricated using conventional screen-printing equipment. Reproduced with permission from ref 56. Copyright 2009 The Japan Society of Applied Physics. (d) A vacuum evaporation machine with a metal cylinder wrapped in an organic transistor active matrix (left), and manufactured organic transistor arrays (right). A magnified image shows the active matrix patterned using a screen-printed shadow mask. Reproduced with permission from ref 57. Copyright 2007 American Institute of Physics.

appropriate for the mass-production of OFETs. However, possible damages to the bottom layers should be avoided during consecutive transfer process. Two types of transfer printing method are available, depending on the phase of the material being transferred. One method involves physical mass transfer between two intrinsically different substrates, and the other involves an embossed/engraved roll for transferring ink. The former method includes soft lithography, such as microcontact or -transfer printing (μCP or μTP). Elastomeric stamps, such as polydimethylsiloxane (PDMS), are typically used as the transfer medium, but rigid stamps, such as silicon wafers or glass, may also be used.[58] Laser-induced forward transfer (LIFT), in which laser irradiation is used to apply a vapor pressure and induce mass transfer, is included in the former category. In the following section, printing processes that rely on μCP, μTP, and LIFT will be briefly introduced, and applications of these processes to the production of OFETs will be reviewed. The last portion of the discussion will also address transfer printing using an embossed/engraved roll (i.e., gravure, flexographic, offset printing), with special attention to the mass production of OFETs via roll-to-roll processes.

3.1. Microcontact and Microtransfer Printing (μCP and μTP). Microcontact printing (μCP), best known as soft lithographic patterning, was invented by Whitesides et al. in the early 1990s.[59] This remarkably simple patterning technique involves inking and stamping processes (Figure 9a).[58] Flexible elastomeric materials, such as PDMS, are commonly used as stamps to ensure conformal contact between the stamp and the receiver substrate; however, rigid stamps may be used for the dry transfer of an active layer to avoid deleterious solvent effects. The stamp's surface chemistry and adhesion between the ink layer and the receiving substrate are key factors that must be optimized to achieve successful printing. In μTP, a functional layer precoated onto one substrate may be picked up

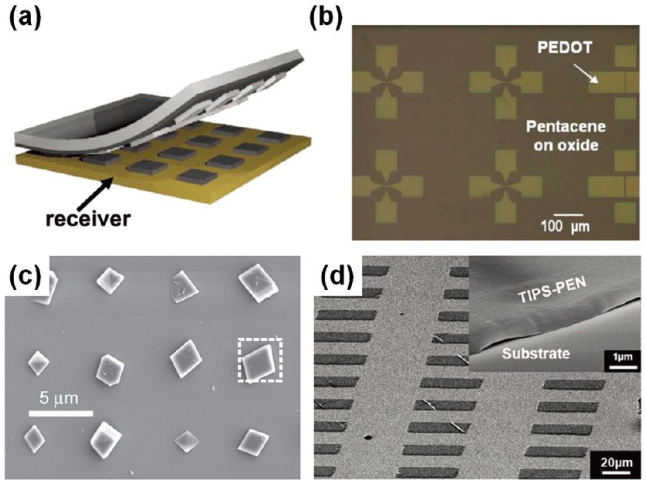

Figure 9. (a) Schematic drawing of the stamping process used for selective printing on a receiver substrate. Reproduced with permission from ref 58. Copyright 2012 Wiley. (b) PEDOT:PSS electrode patterns transferred onto a SiO_2 substrate in the preparation of a bottom-contact OFET. The gap width was varied from 2 to 10 μm. Reproduced with permission from ref 65. Copyright 2006 American Institute of Physics. (c) Patterned pentacene single-crystal array. The dotted squares in the image indicate the size and position of one of the OTS-stamped domains (with a stamped domain size of 4×4 μm^2). Reproduced with permission from ref 76. Copyright 2006 Nature Publishing Group. (d) Tailored TIPS-pentacene single crystals prepared via selective contact evaporation printing. The magnified image in the inset displays the smooth edges of a microdomain. Reproduced with permission from ref 77. Copyright 2011 Wiley.

by a rigid or elastomeric stamp and transferred to a target substrate.[60,61] The scale of the pattern size determines whether a technique is μTP or nTP. The adhesion energies between the donor and receiver substrates need to be carefully optimized via chemical functionalization. The adhesion strength may be described using the Dupré equation $E^{AB}=\gamma_A+\gamma_B-\gamma_{AB}$, where E^{AB} is the interfacial binding energy between materials A and B, $\gamma_{A(B)}$ is the surface free energy of A(B), and γ_{AB} is the interfacial free energy.[62,63] Material C will be transferred from substrate A to substrate B if the following criterion holds: $E^{AC} > E^{BC}$. $E^{A(B)C}$ may be calculated according to the dispersive and polar components of the surface tension. Broadly speaking, two materials with strongly dispersive (hydrophobic) or strongly polar (hydrophilic) surface tension components are likely to adhere with a high adhesion strength. Several exceptions to this principle have been identified. For example, Au adheres weakly to hydrophilic SiO_2 surfaces, even though Au includes highly polarizable electrons. A full understanding of the adhesion phenomena at an interface between donor and receiver substrates therefore relies on extrinsic parameters (the surface roughness, temperature, and pressure) and the surface chemistry at the interface.

μCP or μTP have been used to fabricate OFET functional layers, such as gate electrode, S/D electrodes, gate dielectric, and semiconducting layers. Rogers and co-workers reported the contact printing of metal patterns with nanometer features over large areas.[64] They generated hydroxyl (−OH) groups on a substrate and a metal-coated stamp using oxygen plasma, thereby facilitating a condensation reaction at the (−OH)-bearing interface during contact. This reaction resulted in permanent Ti−O−Si bonds at the interface, preventing delamination of the metal film during stamp detachment. Metal patterns were used to prepare the S/D electrodes in a bottom-contact OFET with a pentacene semiconducting layer. The resultant device exhibited a field-effective mobility of 0.1 $cm^2\ V^{-1}\ s^{-1}$ and an on−off current ratio of $\sim 1.2 \times 10^4$. These values are comparable to the properties of a top-contact transistor fabricated with conventional shadow-mask gold electrodes. In a similar approach, μCP of PEDOT:PSS S/D electrodes yielded a device that performed as well as or better than thermally evaporated metal electrodes. Li et al. reported the preparation of OFETs using PEDOT:PSS S/D electrodes fabricated by μCP (Figure 9b).[65] A channel length of 2 μm was achieved, and the electrical characteristics of the top-contact pentacene OFETs with PEDOT:PSS electrodes (field-effect mobility of 0.3−0.7 $cm^2\ V^{-1}\ s^{-1}$) were superior to those obtained with Au electrodes (field-effect mobility of $\sim 1 \times 10^{-2}$ $cm^2\ V^{-1}\ s^{-1}$) due to a lower carrier injection barrier. Takakuwa et al. conducted the sequential μCP of P3HT and PEDOT:PSS in the preparation of top-contact OFETs.[66] The performances of the resultant devices were enhanced compared with those of spin-cast P3HT films. This improvement was attributed to the high crystallinity of the contact printed P3HT films. Lee and co-workers replaced the PDMS stamp with a rigid glass substrate for the μCP of a P3HT film.[67] The authors attributed the improved device performances to the avoidance of deleterious solvent effects on the underlying dielectric layer during spin-casting of the active film. μTP techniques have also been applied toward device fabrication.[68−70] Williams and co-workers used a Si substrate to transfer OFET components onto plastic substrates.[61] Their transfer printing method permitted the fabrication of each component in an OFET. Other active materials, such as CNTs, may also be transferred using this technique.

μCP of alkylsilane or thiol-based ink was used to fabricate organic transistors by confining molecular self-assembly on the substrate. The fabrication of self-assembled monolayers (SAMs) using thiol-based compounds deposited onto noble metal (Au, Ag, Pt, Pd, and Cu) substrates or using alkylsilane compounds deposited on metal oxide substrates has been extensively studied.[71] Rogers and co-workers patterned electrodes on a plastic substrate using a μ-contact-printed SAM as an etching mask.[72] Etching of the gold substrate not protected by the SAM produced a conducting circuit pattern. This method was used to successfully fabricate high-resolution ($\sim$1 μm) circuits with low levels of defects and good registration over large areas. SAMs enable the surface energy to be controlled by introducing functional groups on the alkyl spacer to achieve selective surface wetting or dewetting of a spin-cast film.[73] Jen and co-workers fabricated a densely packed highly ordered SAM dielectric layer using a combination of μCP of a patterned fluorinated phosphonate and the spin-casting of a long alkylated phosphonate.[74] Rapid SAM formation techniques were used to apply an all-additive patterning approach to the preparation of SAM/metal oxide hybrid dielectrics, providing exceptional dielectric properties and a surface energy that permitted subsequent patterning of solution-processed n-channel and p-channel organic semiconductors. Knipp and co-workers developed a universal microstructuring approach that combined μCP and selective dewetting/wetting.[75] Self-assembled monolayers (SAMs) were patterned on glass or silicon substrates via μCP. The SAM-coated regions were hydrophobic, whereas the uncoated regions remained hydrophilic. Such functionalized surfaces facilitate the selective deposition of polymers or resists. The resist was subsequently used to lift off metallic micro-

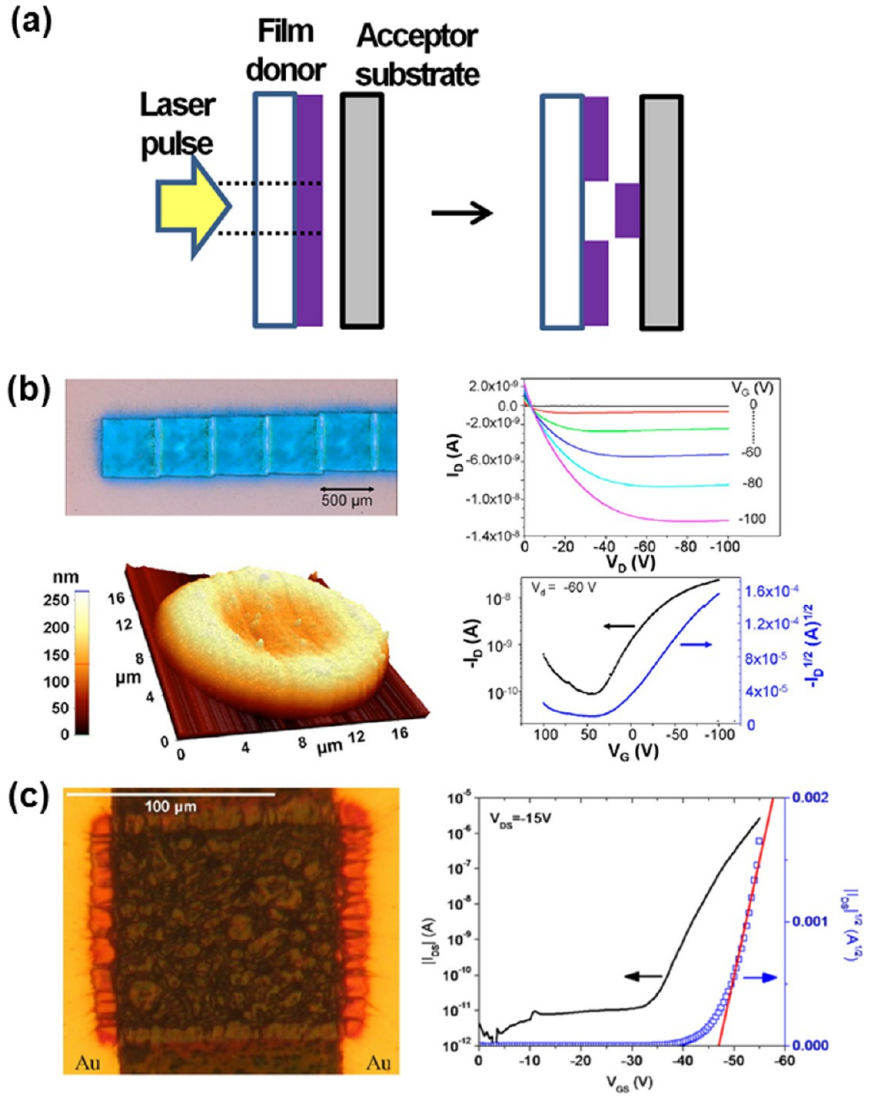

Figure 10. (a) Schematic representation of the laser-induced forward transfer (LIFT) process. (b) LIFT-printed CuPc layer juxtaposed with 500 × 500 μm^2 spots (left/top), and a LIFT pixel of a silver nanoparticle ink after curing (AFM image, left/bottom). The output (right/top) and transfer (right/bottom) characteristics of top-contact OFETs prepared with a CuPc active layer and silver nanoparticle ink electrodes printed by LIFT. Reproduced with permission from ref 85. Copyright 2009 American Institute of Physics. (c) OM image (left) and transfer characteristics (right) of the LIFT-printed P3HT OFETs. Reproduced with permission from ref 86. Copyright 2011 Elsevier.

structures to prepare S/D electrodes in OFETs. Bao and co-workers used μ-contact-printed SAMs to effectively pattern large arrays of single-crystal organic semiconductors (Figure 9c).[76] They found that rough patterned OTS SAMs provided control over the nucleation of vapor-grown organic single crystals. This allowed for the fabrication of large arrays of organic single-crystal field-effect transistors with mobilities as high as 2.4 cm^2 V^{-1} s^{-1} and on−off current ratios greater than 1 × 10^7.

Contrasting with the additive transfer methods described above, subtraction of a target material by μCP has also been demonstrated. This approach, subtractive transfer, involves using a stamp to selectively retrieve regions of a blanket film.[68] This printing modality can be used to directly pattern an active layer or fabricate masks for subsequent processing. Park and co-workers reported the fabrication of TIPS-pentacene single crystal micropatterns, the size and shape of which could be tailored by selective etching of TIPS-pentacene molecules in the region in contact with the topographic PDMS mold, as shown in Figure 9d.[77] Arrays of OFETs with micropatterned TIPS-pentacene single crystal channels exhibited reliable device performance with an on−off current ratio and field-effect mobility of approximately 1 × 10^6 and 0.36 cm^2 V^{-1} s^{-1}, respectively.

3.2. Laser-Induced Forward Transfer (LIFT). Lasers may be used to transfer a thin layer of a donor material to an acceptor substrate. Laser-induced forward transfer (LIFT) processes, developed by Bohandy in 1986,[78] used a pulsed laser beam to heat a donor film, such as a metal layer, on a glass support. Heating converted the glass components into a gaseous state at the glass/metal interface, thereby blasting the metal layer off of the glass support under the intrinsic pressure differential between the metal and the glass (Figure 10a).[79] Similar to OVJP, LIFT is also free from the solvent orthogonality problem. However, it should be noted that possible laser damage should be avoided for the effective function of the devices. LIFT provides for the efficient deposition of a variety of materials, including metals,[80]

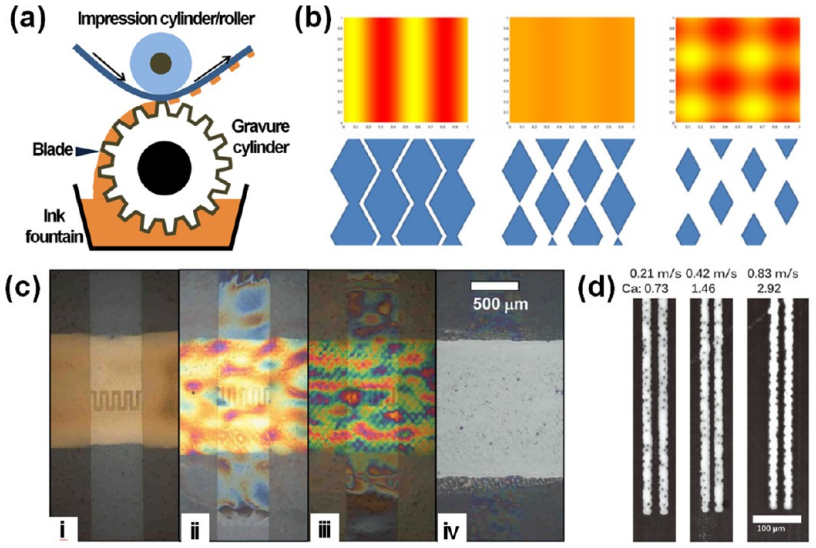

Figure 11. (a) Schematic illustration of the gravure printing process. (b) Schematic diagram showing the film thickness (top) and the equivalent gravure cell volume (bottom) in gravure printed PBTTT films. Reproduced with permission from ref 94. Copyright 2010 Elsevier. (c) Sequential gravure printing of the transistor: (i) the P3HT layer; (ii) after the addition of the PHEMA layer, (iii) after the cross-linking of the XL-PHEMA layer, (iv) and after deposition of the Ag ink gate. Reproduced with permission from ref 95. Copyright 2010 Wiley. (d) Sub-10 μm Ag nanoparticle patterns were prepared using a femtoliter gravure printing process at different printing speeds. Reproduced with permission from ref 97. Copyright 2012 Wiley.

biomaterials,[81] powder,[82] liquids,[83] nanotubes,[84] or organic materials.[85] Ackermann and co-workers used this method to deposit Ag nanoparticle ink to form S/D electrodes and copper phthalocyanine (CuPc) to form an active layer (Figure 10b).[85] The presence of laterally well-resolved square deposits and the lack of damage to the electrode lines indicate that the LIFT process is efficient and precise. AFM investigations revealed that the entire deposition surface was homogeneous. The resultant top-contact device exhibited a field-effect mobility of 8×10^{-5} cm^2 V^{-1} s^{-1}, and an on−off current ratio of 1×10^2.

In addition to organic small molecules and metal films, polymeric semiconductors have been used in the LIFT process. Zergioti and co-workers fabricated a P3HT film using the LIFT process, yielding an average FET field-effect mobility as high as 0.34 cm^2 V^{-1} s^{-1} (Figure 10c).[86] The authors claimed that the thermal energy absorbed by the P3HT during laser irradiation improved both the structural properties of the transferred P3HT and the polymer−SiO_2 interfacial properties. LIFT was applied to a polymer dielectric layer by C. V.-Ackermann and co-workers to fabricate top-gate OFETs.[87] A PMMA insulating polymer layer was spin-coated onto a quartz substrate and transferred by laser onto a CuPc layer that had been deposited previously via vapor phase deposition. The resulting transistors yielded a carrier mobility of 8.6×10^{-3} cm^2 V^{-1} s^{-1}. Notwithstanding the versatile uses of the LIFT process, laser irradiation can induce damage in organic semiconductors.[88] To avoid these problems, Rapp and co-workers deposited a sacrificial layer of Au or triazene polymer to protect the layer from direct irradiation.[89]

3.3. Gravure Printing. Gravure printing is an intaglio printing technique in which ink is carried from an ink fountain to a printing surface using an engraved cylinder (gravure cylinder) (Figure 11a).[90,91] The cylinder comprises periodic cells filled with ink, and the excess is scraped off the surface using a doctor blade. A printing substrate is placed between the rubber-covered impression cylinder and the gravure cylinder containing ink in the cells. As the two cylinders are rotated, they pattern the ink onto a printing substrate. The use of gravure in OFET printing is attractive because it is high-throughput, permits control over the feature size, and is flexible in terms of the substrate selection.[91−93] The printing plate/ink/substrate temperature can be controlled to optimize the printed features. The width and thickness of the printed features depend on the width and depth of the engravings in the mold, the printing speed, the ink viscosity, and the ink/substrate surface energies. Vornbrock and co-workers investigated the dependence of the poly(2,5-bis(3-alkylthiophen-2-yl)thieno-[3,2-b]thiophene) (PBTTT) thin film thickness as a function of the gravure cell volume (Figure 11b).[94] Patterns printed using a high cell volume (21 or 23 mL/m^2) exhibited an oscillatory thickness perpendicular to the print direction but good uniformity along the print direction (Figure 11b/left). By contrast, patterns printed with a low cell volume (6 and 8 mL/m^2) showed incomplete film coverage because the wells were spaced too far apart to permit the ink to spread and merge. Patterns prepared with a slightly higher cell volume (10 mL/m^2) were continuous but exhibited similar color oscillations as are observed among dithered patterns (Figure 11b/right), whereas some cell volumes (13 and 15.6 mL/m^2) yielded optically uniform films (Figure 11b/center). Inkjet-printed silver S/D and gate electrodes were used in gravure-printed PBTTT OFETs, which exhibited a reasonable saturation mobility of 0.06 cm^2 V^{-1} s^{-1} and a modest on−off ratio of 1×10^3. Voigt et al. systematically investigated sequential gravure printing processes for the fabrication of OFETs.[95] Plastic substrates were patterned with ITO S/D contacts, and four different layers were sequentially gravure printed: P3HT, two insulator layers, and an Ag gate (Figure 11c). In the consecutive gravure printing processes, the insulator layer printing processes pose several challenges because they require the successful printing of both an active layer and the S/D contacts. The authors successfully demonstrated gravure-printed OFETs using a poly(2-hydroxyethyl methacrylate) (PHEMA)/cross-linked (XL) PHEMA bilayer dielectric. The best transistor

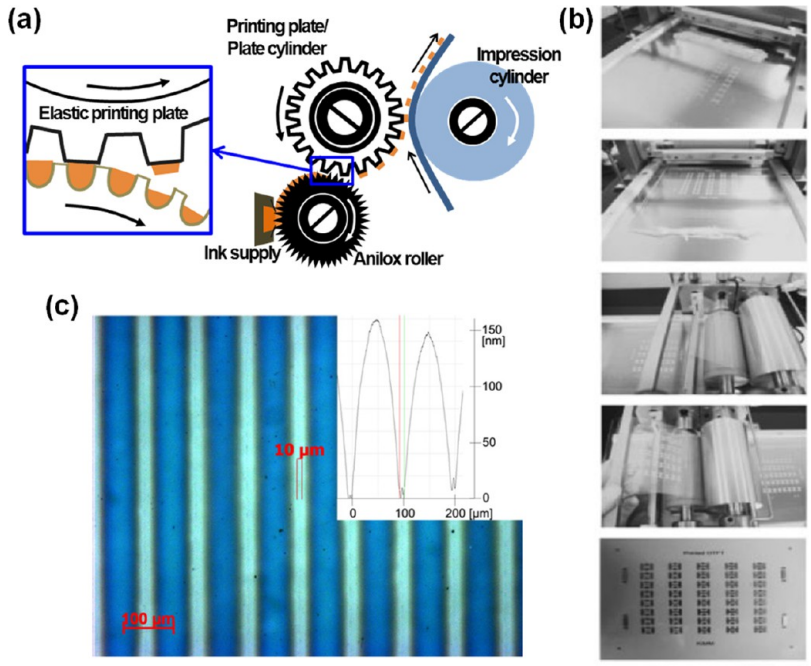

Figure 12. (a) Schematic drawing of the flexography printing process. (b) Photographs of a flexography printing machine used for the fabrication of roll-printed OFETs. Reproduced with permission from ref 98. Copyright 2009 The Japan Society of Applied Physics. (c) OM image of PEDOT:PSS source/drain electrodes fabricated using a Cyflex printing process (flexography+gravure). The inset shows the structure profiles. Reproduced with permission from ref 99. Copyright 2010 Elsevier.

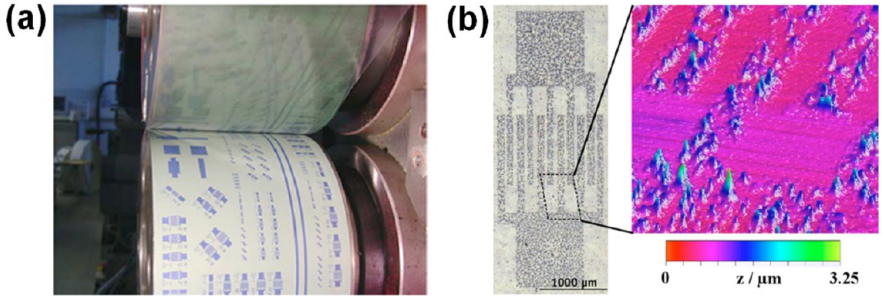

Figure 13. (a) Photograph of an offset printing machine used to produce (b) offset printed PEDOT:PSS S/D electrodes on PET. Both panels reproduced with permission from ref 101. Copyright 2005 American Institute of Physics.

performance, achieved using the P3HT/PHEMA/XL-PHEMA/Ag ink, was 0.04 $cm^2\ V^{-1}\ s^{-1}$ with an on−off current ratio of 1×10^4, rivaling the best top-gate polymer FETs fabricated using these materials.

One important figure of merit for OFET performance is the transition frequency, which represents an upper limit of the device performances. Higher transition frequencies and good AC characteristics require reduced spacings between the S/D electrodes the minimization of the overlap capacitance resulting from the large gate electrodes.[96] Recently, Subramanian and co-workers described the preparation of high-performance OFETs with sub-10 μm metal patterns, prepared using femtoliter gravure printing.[97] In this report, the authors systematically investigated how the rheological parameters of the ink affected the printed features in the gravure printing. A high viscosity and a high printing speed increased the capillary number of the ink, thereby improving the printability of the ink and the electrode patternability, down to 10 μm. (Figure 11d). The PBTTT FETs fabricated with gravure printed S/D and gate electrodes exhibited a high mobility of 0.1 $cm^2\ V^{-1}\ s^{-1}$.

3.4. Flexographic Printing. Flexographic printing, often abbreviated as flexo, is a relief printing technique analogous to a modern version of the letter press. It can be used to print materials onto almost any type of substrate, including plastic, metal, and paper. In this printing process, ink may be transferred from the ink supply to an anilox roll using textures that held a specific amount of ink (Figure 12a). The reliefs on the elastic printing plate picked out a controlled amount of ink from the anilox roll. The ink was subsequently printed onto the printing substrate by passing the substrate through an impression cylinder. Jo et al. reported the preparation of roll-printed electrodes in OFETs using flexographic printing (Figure 12b).[98] The printed OFETs prepared with channels as small as 16 μm were fabricated on a variety of plastic substrates without introducing pattern defects. The device, prepared using the PVP dielectric and TIPS-pentacene semiconductor, then yielded a field-effect mobility of 0.08 $cm^2\ V^{-1}\ s^{-1}$ and an on−off current ratio of about 1×10^5. Combining flexography with other printing techniques may provide an alternative to roll-to-roll OFET fabrication. Hüebler and co-workers demonstrated the flexographic printing of

dx.doi.org/10.1021/am302796z | ACS Appl. Mater. Interfaces 2013, 5, 2302−2315

OFETs wherein flexography was combined with gravure and offset printing.[99] The combined flexography and gravure method (Cyflex) yielded smooth and homogeneous PEDOT:PSS S/D electrodes with a channel length of 10 μm (Figure 12c). Impressively, Facchetti and co-workers reported the preparation of high-mobility n-type polymer OFETs using the flexographic printing of the semiconductor layer and gravure printing of the polymer dielectric layer.[100] They were furthermore able to fabricate inverters by connecting the n-type polymer OFET with a gravure printed P3HT p-type OFET. This fabrication technique appears to be promising for the mass production of OFETs.

3.5. Offset Printing. Offset printing, also referred to as offset lithography, is a printing technique commonly used in commercial printers. The term, "offset", refers to a feature of the process in which the ink is not directly pressed onto the printing surface but is, instead, distributed from a metal plate to an intermediary surface, such as a rubber blanket, then to the printing surface. Compared gravure or flexographic printing, offset printing does not require a texture to be present in relief, rather, offset printing takes advantage of the repulsion between oil and water. On a flat image carrier, an image to be printed (oleophilic region) obtains ink from the ink roller, whereas the nonprinting areas (oleophobic region) attract a water-based film, thereby keeping the nonprinting areas ink-free. Zielke et al. investigated the use of offset printing to prepare S/D electrodes in the production of top-gate OFETs (Figure 13).[101] Offset-printed PEDOT:PSS patterns on a PET foil yielded a conductivity of 30 S/cm, based on a gap width of 50 μm and a line width as small as 100 μm. The fabricated OFETs exhibited a field-effect mobility up to 3×10^{-3} cm^2 V^{-1} s^{-1} and an on−off current ratio of about 1×10^3. Choi et al. succeeded in fabricating electrode features 10 μm in width and 6 μm in spacing, dimensions that were finer than those reported previously.[102] Control over the etching method and the surface energy of the blanket resulted in high-resolution ink transfer. This printing process was used to prepare top-gate amorphous inorganic FETs with short channel lengths.

4. CONCLUSIONS AND FUTURE RESEARCH PERSPECTIVES

We have reviewed the recent achievements in OFET printing processes. In an effort to achieve the large-area/high-throughput patterning of active components in OFETs, a variety of fabrication techniques have been developed. Over the past two decades, new functional materials have been synthesized, and the OFET device physics have become better understood. Material and theoretical improvements have dramatically enhanced the field-effect mobilities of OFETs from 1×10^{-5} cm^2 V^{-1} s^{-1} to 30 cm^2 V^{-1} s^{-1}.[20] Aside from new development of materials and device structures, the processing methods also significantly affect the device performances of OFETs by changing morphologies and structural ordering of the organic semiconductor films. In this regard, double shot inkjet printing process or digital-mode OVJP method, which has shown opportunity to control the properties of organic semiconductor films, will be alternative route for fabricating high performance OFETs. In addition, several consecutive printing processes such as sequential gravure printing and flexography will provide processing technology for mass production of OFETs. These results guarantee a bright future for OFETs.

However, the printing processes used to prepare OFETs must be further developed before they may be commercialized. For the high performance OFETs, the control of the molecular orientation and film morphologies of organic semiconductors should be more optimized. A solution shearing method recently developed by Bao and co-workers showed possibility to control the $\pi-\pi$ stacking distance by incrementally introducing lattice strain.[103] Their method altered the $\pi-\pi$ stacking distance of TIPS-pentacene from 3.33 to 3.08 Å while achieving a high mobility of 4.6 cm^2 V^{-1} s^{-1}. This result suggests that printing process can be more advantageous both in device performance and production yield than conventional processing methods such as spin-casting or drop-casting.[104] Another requirement for the production of OFETs is reducing pattern size. To achieve high spatial resolution, recently developed patterning method such as liquid bridge-mediated nanotransfer molding may provide alternative for printed electronics in the near future.[105] Fabrication of two- or three-dimensional structures with feature sizes as small as tens of nanometers was demonstrated over large areas. We believe that a new printing process that is simultaneously low-cost, high-throughput, and yields high device performances will be additionally developed in the near future. The advances in printing processes support the realization of mass-produced high-performance OFETs.

AUTHOR INFORMATION

Corresponding Author

*E-mail: kwcho@postech.ac.kr (K.C.), whlee78@konkuk.ac.kr (W.H.L.). Tel: 82-54-279-2270. Fax: 82-54-279-8298.

Notes

The authors declare no competing financial interest.

ACKNOWLEDGMENTS

This work was supported by grants from the Leading Foreign Research Institute Recruitment Program (2010-00525) and the Center for Advanced Soft Electronics under the Global Frontier Research Program (2011-0031628) of the Ministry of Education, Science and Technology, Korea.

REFERENCES

(1) Moonen, P. F.; Yakimets, I.; Huskens, J. *Adv. Mater.* **2012**, *24*, 5526−5541.
(2) Carlson, A.; Bowen, A. M.; Huang, Y.; Nuzzo, R. G.; Rogers, J. A. *Adv. Mater.* **2012**, *24*, 5284−5318.
(3) Tobjork, D.; Osterbacka, R. *Adv. Mater.* **2011**, *23*, 1935−1961.
(4) Berggren, M.; Nilsson, D.; Robinson, N. D. *Nat. Mater.* **2007**, *6*, 3−5.
(5) Forrest, S. R. *Nature* **2004**, *428*, 911−8.
(6) Cho, J. H.; Lee, J.; Xia, Y.; Kim, B.; He, Y.; Renn, M. J.; Lodge, T. P.; Frisbie, C. D. *Nat. Mater.* **2008**, *7*, 900−906.
(7) Sirringhaus, H.; Kawase, T.; Friend, R. H.; Shimoda, T.; Inbasekaran, M.; Wu, W.; Woo, E. P. *Science* **2000**, *290*, 2123−2126.
(8) Yoon, M. H.; Yan, H.; Facchetti, A.; Marks, T. J. *J. Am. Chem. Soc.* **2005**, *127*, 10388−10395.
(9) Jang, Y.; Kim, D. H.; Park, Y. D.; Cho, J. H.; Hwang, M.; Cho, K. W. *Appl. Phys. Lett.* **2005**, *87*, 152105−152107.
(10) Noh, Y. Y.; Zhao, N.; Caironi, M.; Sirringhaus, H. *Nat. Nanotechnol.* **2007**, *2*, 784−789.
(11) Qiu, L. Z.; Xu, Q.; Lee, W. H.; Wang, X. H.; Kang, B.; Lv, G. Q.; Cho, K. *J. Mater. Chem.* **2011**, *21*, 15637−15642.
(12) Lee, W. H.; Cho, J. H.; Cho, K. *J. Mater. Chem.* **2010**, *20*, 2549−2561.
(13) Park, Y. D.; Lee, H. S.; Choi, Y. J.; Kwak, D.; Cho, J. H.; Lee, S.; Cho, K. *Adv. Funct. Mater.* **2009**, *19*, 1200−1206.

(14) Kim, D. H.; Park, Y. D.; Jang, Y. S.; Yang, H. C.; Kim, Y. H.; Han, J. I.; Moon, D. G.; Park, S. J.; Chang, T. Y.; Chang, C. W.; Joo, M. K.; Ryu, C. Y.; Cho, K. W. *Adv. Funct. Mater.* **2005**, *15*, 77−82.
(15) Singh, M.; Haverinen, H. M.; Dhagat, P.; Jabbour, G. E. *Adv. Mater.* **2010**, *22*, 673−685.
(16) Deegan, R. D.; Bakajin, O.; Dupont, T. F.; Huber, G.; Nagel, S. R.; Witten, T. A. *Nature* **1997**, *389*, 827−829.
(17) Lim, J. A.; Lee, H. S.; Lee, W. H.; Cho, K. *Adv. Funct. Mater.* **2009**, *19*, 1515−1525.
(18) James, D. T.; Kjellander, B. K. C.; Smaal, W. T. T.; Gelinck, G. H.; Combe, C.; McCulloch, I.; Wilson, R.; Burroughes, J. H.; Bradley, D. D. C.; Kim, J. S. *ACS Nano* **2011**, *5*, 9824−9835.
(19) Lim, J. A.; Lee, W. H.; Lee, H. S.; Lee, J. H.; Park, Y. D.; Cho, K. *Adv. Funct. Mater.* **2008**, *18*, 229−234.
(20) Minemawari, H.; Yamada, T.; Matsui, H.; Tsutsumi, J.; Haas, S.; Chiba, R.; Kumai, R.; Hasegawa, T. *Nature* **2011**, *475*, 364−367.
(21) Lim, J. A.; Lee, W. H.; Kwak, D.; Cho, K. *Langmuir* **2009**, *25*, 5404−5410.
(22) Kim, Y. H.; Yoo, B.; Anthony, J. E.; Park, S. K. *Adv. Mater.* **2012**, *24*, 497−502.
(23) Kjellander, B. K. C.; Smaal, W. T. T.; Anthony, J. E.; Gelinck, G. H. *Adv. Mater.* **2010**, *22*, 4612−4616.
(24) Yan, H.; Chen, Z.; Zheng, Y.; Newman, C.; Quinn, J. R.; Dotz, F.; Kastler, M.; Facchetti, A. *Nature* **2009**, *457*, 679−686.
(25) Khim, D.; Lee, W. H.; Baeg, K. J.; Kim, D. Y.; Kang, I. N.; Noh, Y. Y. *J. Mater. Chem.* **2012**, *22*, 12774−12783.
(26) Kim, D, H.; Shin, H. J.; Lee, H. S.; Lee, J.; Lee, B. L.; Lee, W. H.; Lee, J. H.; Cho, K.; Kim, W. J.; Lee, S. Y.; Choi, J. Y.; Kim, J. M. *ACS Nano* **2012**, *6*, 662−670.
(27) Lim, J. A.; Kim, J. H.; Qiu, L.; Lee, W. H.; Lee, H. S.; Kwak, D.; Cho, K. *Adv. Funct. Mater.* **2010**, *20*, 3292−3297.
(28) Qiu, L. Z.; Lee, W. H.; Wang, X. H.; Kim, J. S.; Lim, J. A.; Kwak, D.; Lee, S.; Cho, K. *Adv. Mater.* **2009**, *21*, 1349−1353.
(29) Madec, M. B.; Smith, P. J.; Malandraki, A.; Wang, N.; Korvink, J. G.; Yeates, S. G. *J. Mater. Chem.* **2010**, *20*, 9155−9160.
(30) Wang, J. Z.; Zheng, Z. H.; Li, H. W.; Huck, W. T.; Sirringhaus, H. *Nat. Mater.* **2004**, *3*, 171−176.
(31) Sele, C. W.; von Werne, T.; Friend, R. H.; Sirringhaus, H. *Adv. Mater.* **2005**, *17*, 997−1001.
(32) Lim, J. A.; Cho, J. H.; Park, Y. D.; Kim, D. H.; Hwang, M.; Cho, K. *Appl. Phys. Lett.* **2006**, *88*, 082102−082104.
(33) Wu, Y. L.; Li, Y. N.; Ong, B. S.; Liu, P.; Gardner, S.; Chiang, B. *Adv. Mater.* **2005**, *17*, 184−187.
(34) Gamerith, S.; Klug, A.; Scheiber, H.; Scherf, U.; Moderegger, E.; List, E. J. W. *Adv. Funct. Mater.* **2007**, *17*, 3111−3118.
(35) Woo, K.; Bae, C.; Jeong, Y.; Kim, D.; Moon, J. *J. Mater. Chem.* **2010**, *20*, 3877−3882.
(36) Kim, D.; Jeong, S.; Shin, H.; Xia, Y.; Moon, J. *Adv. Mater.* **2008**, *20*, 3084−3089.
(37) Ko, S. H.; Pan, H.; Grigoropoulos, C. P.; Luscombe, C. K.; Frechet, J. M. J.; Poulikakos, D. *Nanotechnology* **2007**, *18*, 345202−345209.
(38) Sekitani, T.; Noguchi, Y.; Zschieschang, U.; Klauk, H.; Someya, T. *Proc. Natl. Acad. Sci. U.S.A.* **2008**, *105*, 4976−4980.
(39) Hecht, D. S.; Hu, L. B.; Irvin, G. *Adv. Mater.* **2011**, *23*, 1482−1513.
(40) Torrisi, F.; Hasan, T.; Wu, W. P.; Sun, Z. P.; Lombardo, A.; Kulmala, T. S.; Hsieh, G. W.; Jung, S. J.; Bonaccorso, F.; Paul, P. J.; Chu, D. P.; Ferrari, A. C. *ACS Nano* **2012**, *6*, 2992−3006.
(41) Lim, S.; Kang, B.; Kwak, D.; Lee, W. H.; Lim, J. A.; Cho, K. *J. Phys. Chem. C* **2012**, *116*, 7520−7525.
(42) Zhang, L.; Liu, H. T.; Zhao, Y.; Sun, X. N.; Wen, Y. G.; Guo, Y. L.; Gao, X. K.; Di, C. A.; Yu, G.; Liu, Y. Q. *Adv. Mater.* **2012**, *24*, 436−440.
(43) Eda, G.; Chhowalla, M. *Adv. Mater.* **2010**, *22*, 2392−2415.
(44) Loh, K. P.; Bao, Q. L.; Ang, P. K.; Yang, J. X. *J. Mater. Chem.* **2010**, *20*, 2277−2289.
(45) Park, S.; Ruoff, R. S. *Nat. Nanotechnol.* **2009**, *4*, 217−224.
(46) Jang, Y.; Park, Y. D.; Lim, J. A.; Lee, H. S.; Lee, W. H.; Cho, K. *Appl. Phys. Lett.* **2006**, *89*, 183501−183503.
(47) Chan, C. K.; Richter, L. J.; Dinardo, B.; Jaye, C.; Conrad, B. R.; Ro, H. W.; Germack, D. S.; Fischer, D. A.; DeLongchamp, D. M.; Gundlach, D. J. *Appl. Phys. Lett.* **2010**, *96*, 133304−133306.
(48) Shtein, M.; Peumans, P.; Benziger, J. B.; Forrest, S. R. *Adv. Mater.* **2004**, *16*, 1615−1620.
(49) Shtein, M.; Peumans, P.; Benziger, J. B.; Forrest, S. R. *J. Appl. Phys.* **2004**, *96*, 4500−4507.
(50) Yun, C.; Choi, J.; Kang, H. W.; Kim, M.; Moon, H.; Sung, H. J.; Yoo, S. *Adv. Mater.* **2012**, *24*, 2857−2862.
(51) Chen, J. L.; Leblanc, V.; Kang, S. H.; Benning, P. J.; Schut, D.; Baldo, M. A.; Schmidt, M. A.; Bulovic, V. *Adv. Funct. Mater.* **2007**, *17*, 2722−2727.
(52) Pardo, D. A.; Jabbour, G. E.; Peyghambarian, N. *Adv. Mater.* **2000**, *12*, 1249−1252.
(53) Garnier, F.; Hajlaoui, R.; Yassar, A.; Srivastava, P. *Science* **1994**, *265*, 1684−1686.
(54) Bao, Z.; Feng, Y.; Dodabalapur, A.; Raju, V. R.; Lovinger, A. J. *Chem. Mater.* **1997**, *9*, 1299−1301.
(55) Rogers, J. A.; Bao, Z. N.; Raju, V. R. *Appl. Phys. Lett.* **1998**, *72*, 2716−2718.
(56) Lim, S. C.; Kim, S. H.; Yang, Y. S.; Lee, M. Y.; Nam, S. Y.; Bin Ko, J. *Jpn. J. Appl. Phys.* **2009**, *48*, 081503−081505.
(57) Noguchi, Y.; Sekitani, T.; Someya, T. *Appl. Phys. Lett.* **2007**, *91*, 133502−133504.
(58) Carlson, A.; Bowen, A. M.; Huang, Y. G.; Nuzzo, R. G.; Rogers, J. A. *Adv. Mater.* **2012**, *24*, 5284−5318.
(59) Kumar, A.; Biebuyck, H. A.; Abbott, N. L.; Whitesides, G. M. *J. Am. Chem. Soc.* **1992**, *114*, 9188−9189.
(60) Zaumseil, J.; Meitl, M. A.; Hsu, J. W. P.; Acharya, B. R.; Baldwin, K. W.; Loo, Y.-L.; Rogers, J. A. *Nano Lett.* **2003**, *3*, 1223−1227.
(61) Hines, D. R.; Mezhenny, S.; Breban, M.; Williams, E. D.; Ballarotto, V. W.; Esen, G.; Southard, A.; Fuhrer, M. S. *Appl. Phys. Lett.* **2005**, *86*, 163101−163103.
(62) Kinloch, A. J. *Polymer Surfaces and Interfaces*; Wiley: Chichester, U.K., 1987.
(63) Muller, P.; Kern, R. *Surf. Sci.* **2000**, *457*, 229−253.
(64) Loo, Y. L.; Willett, R. L.; Baldwin, K. W.; Rogers, J. A. *Appl. Phys. Lett.* **2002**, *81*, 562−564.
(65) Li, D. W.; Guo, L. J. *Appl. Phys. Lett.* **2006**, *88*, 063513−063515.
(66) Takakuwa, A.; Azumi, R. *Jpn. J. Appl. Phys.* **2008**, *47*, 1115−1118.
(67) Park, J.; Shim, S. O.; Lee, H. H. *Appl. Phys. Lett.* **2005**, *86*, 073505−073507.
(68) Hines, D. R.; Ballarotto, V. W.; Williams, E. D.; Shao, Y.; Solin, S. A. *J. Appl. Phys.* **2007**, *101*, 024503−024511.
(69) Keum, C. M.; Bae, J. H.; Kim, M. H.; Choi, W.; Lee, S. D. *Org. Electron.* **2012**, *13*, 778−783.
(70) Hines, D. R.; Southard, A.; Fuhrer, M. S. *J. Appl. Phys.* **2008**, *104*, 024510−024514.
(71) Ulman, A. *Chem. Rev.* **1996**, *96*, 1533−1554.
(72) Rogers, J. A.; Bao, Z.; Baldwin, K.; Dodabalapur, A.; Crone, B.; Raju, V. R.; Kuck, V.; Katz, H.; Amundson, K.; Ewing, J.; Drzaic, P. *Proc. Natl. Acad. Sci. U.S.A.* **2001**, *98*, 4835−4840.
(73) Ma, H.; Yip, H. L.; Huang, F.; Jen, A. K. Y. *Adv. Funct. Mater.* **2010**, *20*, 1371−1388.
(74) Acton, O.; Hutchins, D.; Arnadottir, L.; Weidner, T.; Cernetic, N.; Ting, G. G.; Kim, T. W.; Castner, D. G.; Ma, H.; Jen, A. K. Y. *Adv. Mater.* **2011**, *23*, 1899−1902.
(75) Benor, A.; Hoppe, A.; Wagner, V.; Knipp, D. *Thin Solid Films* **2007**, *515*, 7679−7682.
(76) Briseno, A. L.; Mannsfeld, S. C. B.; Ling, M. M.; Liu, S. H.; Tseng, R. J.; Reese, C.; Roberts, M. E.; Yang, Y.; Wudl, F.; Bao, Z. N. *Nature* **2006**, *444*, 913−917.
(77) Bae, I.; Kang, S. J.; Shin, Y. J.; Park, Y. J.; Kim, R. H.; Mathevet, F.; Park, C. *Adv. Mater.* **2011**, *23*, 3398−3402.
(78) Bohandy, J.; Kim, B. F.; Adrian, F. J. *J. Appl. Phys.* **1986**, *60*, 1538−1539.

(79) Roder, T. C.; Kohler, J. R. *Appl. Phys. Lett.* **2012**, *100*, 071603−071605.
(80) Bohandy, J.; Kim, B. F.; Adrian, F. J.; Jette, A. N. *J. Appl. Phys.* **1988**, *63*, 1158−1162.
(81) Chrisey, D. B.; Piqué, A.; McGill, R. A.; Horwitz, J. S.; Ringeisen, B. R.; Bubb, D. M.; Wu, P. K. *Chem. Rev.* **2003**, *103*, 553−576.
(82) Kononenko, T. V.; Alloncle, P.; Konov, V. I.; Sentis, M. *Appl. Phys. a-Mater.* **2009**, *94*, 531−536.
(83) Duocastella, M.; Fernandez-Pradas, J. M.; Serra, P.; Morenza, J. L. *Appl. Phys. a-Mater.* **2008**, *93*, 453−456.
(84) Boutopoulos, C.; Pandis, C.; Giannakopoulos, K.; Pissis, P.; Zergioti, I. *Appl. Phys. Lett.* **2010**, *96*, 041104−041106.
(85) Rapp, L.; Diallo, A. K.; Alloncle, A. P.; Videlot-Ackermann, C.; Fages, F.; Delaporte, P. *Appl. Phys. Lett.* **2009**, *95*, 171109−171111.
(86) Zergioti, I.; Makrygianni, M.; Dimitrakis, P.; Normand, P.; Chatzandroulis, S. *Appl. Surf. Sci.* **2011**, *257*, 5148−5151.
(87) Diallo, A. K.; Rapp, L.; Nenon, S.; Alloncle, A. P.; Delaporte, P.; Fages, F.; Videlot-Ackermann, C. *Synth. Met.* **2011**, *161*, 888−893.
(88) Fardel, R.; Nagel, M.; Nuesch, F.; Lippert, T.; Wokaun, A. *Appl. Phys. Lett.* **2007**, *91*, 061103−061105.
(89) Rapp, L.; Cibert, C.; Nenon, S.; Alloncle, A. P.; Nagel, M.; Lippert, T.; Videlot-Ackermann, C.; Fages, F.; Delaporte, P. *Appl. Surf. Sci.* **2011**, *257*, 5245−5249.
(90) Sung, D.; de la Fuente Vornbrock, A.; Subramanian, V. *IEEE Trans. Compon. Packag. Technol.* **2010**, *33*, 105−114.
(91) Yin, X.; Kumar, S. *Chem. Eng. Sci.* **2006**, *61*, 1146−1156.
(92) Schwartz, L. W. *J. Eng. Math.* **2002**, *42*, 243−253.
(93) Kapur, N. *Chem. Eng. Sci.* **2003**, *58*, 2875−2882.
(94) Vornbrock, A. D.; Sung, D. V.; Kang, H. K.; Kitsomboonloha, R.; Subramanian, V. *Org. Electron.* **2010**, *11*, 2037−2044.
(95) Voigt, M. M.; Guite, A.; Chung, D. Y.; Khan, R. U. A.; Campbell, A. J.; Bradley, D. D. C.; Meng, F. S.; Steinke, J. H. G.; Tierney, S.; McCulloch, I.; Penxten, H.; Lutsen, L.; Douheret, O.; Manca, J.; Brokmann, U.; Sonnichsen, K.; Hulsenberg, D.; Bock, W.; Barron, C.; Blanckaert, N.; Springer, S.; Grupp, J.; Mosley, A. *Adv. Funct. Mater.* **2010**, *20*, 239−246.
(96) Tseng, H. Y.; Subramanian, V. *Org. Electron.* **2011**, *12*, 249−256.
(97) Kang, H.; Kitsomboonloha, R.; Jang, J.; Subramanian, V. *Adv. Mater.* **2012**, *24*, 3065−3069.
(98) Jo, J.; Yu, J. S.; Lee, T. M.; Kim, D. S. *Jpn. J. Appl. Phys.* **2009**, *48*, 04C181−04C185.
(99) Schmidt, G. C.; Bellmann, M.; Meier, B.; Hambsch, M.; Reuter, K.; Kempa, H.; Hubler, A. C. *Org. Electron.* **2010**, *11*, 1683−1687.
(100) Yan, H.; Chen, Z. H.; Zheng, Y.; Newman, C.; Quinn, J. R.; Dotz, F.; Kastler, M.; Facchetti, A. *Nature* **2009**, *457*, 679−687.
(101) Zielke, D.; Hubler, A. C.; Hahn, U.; Brandt, N.; Bartzsch, M.; Fugmann, U.; Fischer, T.; Veres, J.; Ogier, S. *Appl. Phys. Lett.* **2005**, *87*, 123508−123510.
(102) Choi, N.; Wee, H.; Nam, S.; Lavelle, J.; Hatalis, M. *Microelectron. Eng.* **2012**, *91*, 93−97.
(103) Giri, G.; Verploegen, E.; Mannsfeld, S. C. B.; Atahan-Evrenk, S.; Kim, D. H.; Lee, S. Y.; Becerril, H. A.; Aspuru-Guzik, A.; Toney, M. F.; Bao, Z. A. *Nature* **2011**, *480*, 504−509.
(104) Lee, J.; Han, A. R.; Kim, J.; Kim, Y.; Oh, J. H.; Yang, C. *J. Am. Chem. Soc.* **2012**, *134*, 20713−20721.
(105) Hwang, J. K.; Cho, S.; Dang, J. M.; Kwak, E. B.; Song, K.; Moon, J.; Sung, M. M. *Nat. Nanotechnol.* **2010**, *5*, 742−748.